

Modeling and Tolerance Analysis of Monolithic InP-based Dual Polarization QPSK Transmitter

Cristina Arellano¹, André Richter¹, Sergei Mingaleev², Igor Koltchanov¹, Christophe Kazmierski³

¹: VPIphotonics GmbH, Carnotstr. 6, 10587 Berlin, Germany

²: VPI Development Center, Chapaveva str. 5, 220034 Minsk, Belarus

³: III-VLab, Route de Nozay, 91460 Marcoussis, France

e-mail: Cristina.Arellano@VPIphotonics.com

Abstract—We present a detailed circuit model for a monolithic integrated InP transmitter and its application for the study of technological limitations such the impact of non-ideal phase shifters and reflections at interfaces.

I. INTRODUCTION

Technological advances in monolithic integration enable the fabrication of complex photonic integrated circuits (PICs) that might comprise a large number of sub-elements performing several tenths of photonic functions. The design and optimization of large-scale PICs gathers speed with the introduction of novel photonic circuit simulators [1-4] that allow rapid functional prototyping without going into fabrication details. Certainly, detailed physical modeling of critical individual sub-elements needs to be done. Then, those results can be easily reused not only for the same PIC design but also in further schemes. The compilation of realistic circuit-level abstracted models evidently accelerates the design process as well as decreases the number of required runs to achieve the final model.

In previous works, we have presented methodologies for modeling fully passive PICs [5]; hybrid PICs, comprising active and clusters of passive PIC elements [6]; and more complex optoelectronic circuits, including also linear electrical elements (EEs) [7]. Within this work we show the power of circuit simulations for the design and analysis of a monolithic integrated InP-based dual polarization QPSK transmitter which has been developed in frame of the European research project MIRTHE [8]. A first detailed analysis of a former transmitter design (single polarization) is reported in [9]. There we studied the effect of nonlinear voltage dependencies of EAMs, jitter and synchronization of driving signals, preliminary analyzed reflections at facets of active elements, and tolerances of MMI dimensions and phase shifters. The results presented here have been obtained using the professional circuit modeling environment *VPIcomponentMaker™ Photonic Circuits*.

II. DETAILED MODEL OF THE TRANSMITTER

Our circuit simulation is based on the segmentation of the modeled PIC into functional building blocks, named PIC elements. The set of PIC elements allowable on the same circuit typically consists of a mix of photonic, electronic or optoelectronic, active or passive functions. Passive photonic PIC elements as well as EEs are well defined by frequency-

dependent transfer functions (S-matrices). Active photonic PIC elements require more sophisticated physical models to account for carrier dynamics, noise generation and other non-linear effects. These are numerically solved in time domain. In a hybrid structure, as is the case of monolithic integrated PICs, we make use of our time-and-frequency domain method (TFDM), which improves the overall speed and accuracy when compared to a pure time-domain simulation using a moderate number of samples [6, 8].

The model of the transmitter is shown in Fig. 1. The layout of the fabricated device is shown as reference below. The device consists of two mirrored single-polarization IQ-transmitters. The signal of the DFB laser is distributed to two modulation sections by means of a 1:2 MMI splitter. The laser model is based on rate equations. It accounts for characteristics such as carrier dynamics, noise, linewidth, chirp, and reflections at end facets. At each of the two blocks, the signal is directed to the four EAMs by a 1:4 MMI splitter. MMI elements allow representing the fabricated sub-elements since the exact geometrical dimensions (length and width) define the element; as well as the locations and widths of input and output ports. Thus, possible fabrication imperfections can be modeled. Between the 1:4 MMI and EAM elements, there are bent waveguide models that account for transmission and bending loss as well as for possible reflections. The EAM model considers the voltage dependences of the peak absorption magnitude, peak absorption frequency and bandwidth as third order polynomials. In that way, nonlinear saturation effects are accounted for in the transmitter model. Chirp and frequency detuning are specified in the model by refractive index-dependence parameters. Each of the four EAMs is followed by a phase shifter with a fixed value of 0°, 180°, 270° and 90° needed for generating the required modulation. The phase shift is accomplished by injecting appropriate currents into the waveguides. The model follows the relationship current-phase shift of the fabricated devices with a nonlinear characteristic. Notice that this requires a very fine tuning of the bias current of the four (eight, considering both polarizations) phase elements after realization of the device. This, together with unwanted current fluctuations might affect not only the phase, but also cause imbalances due to the loss dependency on carrier density. Such effects can be accounted for in the simulations. The four branches of each transmitter block are joined via two stages of 2:1 MMI couplers. The outputs are fed into SOAs for amplification purposes. The rotation of one of the outputs and the combination of both signals for transmission is

accomplished outside of the fabricated chip. The bidirectional characteristic of all PIC elements allows considering reflections from each part of the circuit.

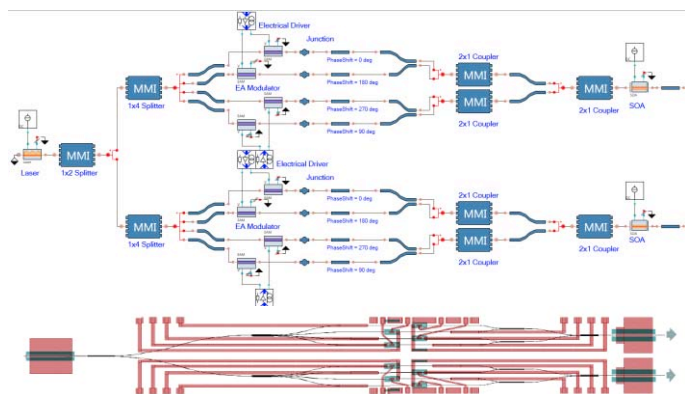


Figure 1. Schematic of the simulated transmitter (top) and layout of the fabricated device (bottom)

III. IMPACT OF NON-OPTIMUM PHASE SHIFTERS

Phase shifting is accomplished by carrier-induced changes in the refractive index of the waveguides, which is inherently a nonlinear effect [10]. Measurement results showed that, indeed, the employed phase shifters exhibit a nonlinear dependence of phase and loss with applied current. As a different phase shift is applied to each of the four branches, fluctuations of applied current from the optimum one will have a different effect on phase and loss offset in each of the four branches. Fig. 2 shows the standard deviation for a QPSK-signal for individual current fluctuations while keeping the other currents at their optimum values. Assuming that a relative variation of constellation points below 1% is acceptable, our results show that I4 (90°) must be kept very close to the optimum value. Further we studied the combined impact of random current fluctuations and we found that current offsets in the individual branches do not cause strictly additive constellation point variations.

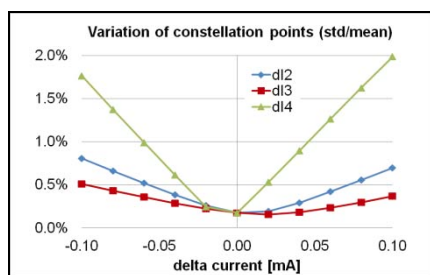


Figure 2. Variation of QPSK constellation points for different current offsets

IV. IMPACT OF REFLECTIONS

Further, we studied the impact of unwanted feedback signals within the transmitter device, paying special attention to reflections at the active-passive material interface and at the output interface of the transmitter. We found that the impact of reflections at the active-passive interface remains constant for different levels of amplification and is slightly lower than the

one caused by reflections at the end of the device. Reflections at the end of the device are enhanced due to re-amplification in the SOA and might be critical for high levels of output power. Consequently, it is generally of high interest to increase the output power of the laser and work on decreasing the loss of passive waveguides and other connecting elements. Additionally, our studies suggested that reflections at the SOA-air interface have a strong impact on the broadening of the laser linewidth (Fig. 3). Further we found that even when the total output power remains constant in average, strong power fluctuations at the laser output may occur, causing increased pattern effects in time-domain of the transmitted output.

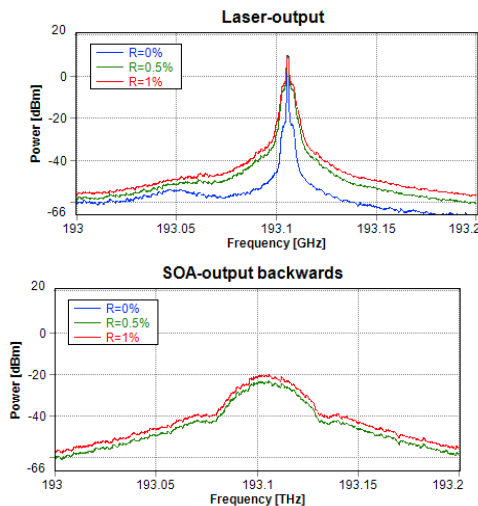


Figure 3. Spectra after laser (top) and backwards into the modulation section (bottom) for different values of reflection

ACKNOWLEDGMENT

This work has been partially funded by the EU FP7/2007-2013 under the grant agreement n° 257980 (MIRTHE).

REFERENCES

- [1] ASPIC, <http://www.aspicdesign.com>
- [2] PICWave, <http://www.photond.com/products/picwave.htm>
- [3] Interconnect, <https://www.lumerical.com/tcad-products/interconnect/>
- [4] VPIcomponentMaker™ Photonic Circuits, <http://vpiphotonics.com/CMPhotonicCircuits.php>
- [5] Arellano, C., Mingaleev, S.F., Sokolov, E., Koltchanov I., Richter A., "Efficient Design of Photonic Integrated Circuits (PICs)," ICTON, paper Th.A4.1 (2011).
- [6] Arellano, C., Mingaleev, S.F., Sokolov, E., Koltchanov I., Richter A., "Time-and-Frequency-Domain Modeling (TFDM) of Hybrid Photonic Integrated Circuits," OPTO Photonics West, paper 8265-19 (2012).
- [7] Arellano, C., Mingaleev, S.F., Sokolov, Richter A., "Modeling of Opto-Electronics in Complex Photonic Integrated Circuits," OPTO Photonics West, paper 8980-61 (2014).
- [8] <http://www.ist-mirthe.eu>
- [9] Richter A., Arellano, C., Mingaleev, S.F., Sokolov, E., Koltchanov I., "Detailed Modeling of Integrated IQ-Transmitters for 100G+ Applications" OPTO Photonics West, paper 82840L (2012).
- [10] B. R. Bennett, R. A. Soref, J. A. del Alamo, "Carrier-Induced Change in Regractive Index of InP, GaAs, and InGaAsP", Journal of Quantum Electr. Vol. 26, No.1, (1990)